Effect of pH on the Synthesis of CuO Nanosheets by Quick Precipitation Method

MAHDI SHAHMIRI[a], NOR AZOWA IBRAHIM[a]*, NORHAZLIN ZAINUDDIN[a], NILOFAR ASIM[b], B BAKHTYAR[b], A ZAHARIM[b], K SOPIAN[b]

[a] Faculty of Science, Universiti Putra Malaysia, 43400 UPM Serdang, Selangor, MALAYSIA
[b] Solar Energy Research Institute, Universiti Kebangsaan Malaysia, 43600 Bangi, Selangor, MALAYSIA
*email: norazowa@science.upm.edu.my

Abstract: In this paper, copper oxide nanosheets were successfully fabricated in polyvinylpyrrolidone (PVP) via a quick precipitation method. The synthesized CuO nanostructures were characterized by X-ray diffraction (XRD), UV-vis spectroscopy, transmission electron microscopy (TEM), field emission scanning electron microscopy, energy dispersive analysis of X-ray, and Fourier transform infrared (FT-IR) spectroscopy. The effect of pH on the final product was investigated. The results show that a higher volume ratio of NaOH results in well-defined CuO nanosheets. XRD results confirmed the formation of pure CuO with a monoclinic structure at higher pH, whereas gerhardtite was formed at lower pH. TEM results indicate that sheet-like CuO were formed at higher pH. FT-IR results show that C=O in PVP coordinated with CuO and formed a protection layer. The generation of CuO nanostructures was proven by UV-vis spectroscopy. The mechanism of the reaction was also discussed.

Keywords: Nanosheets, Nanorods, CuO, quick precipitation, Polyvinylpyrrolidone, orientated attachment mechanism (OA)

1. Introduction

Particles with sizes between 1 and 100 nm are called nanoparticles, which have one or more dimensions. One of the unique properties of nanoparticles is their large surface area-to-volume ratio, which gives them different properties compared with bulk materials that are made from the same substances. The investigation on nanoparticles, which includes fabrication and characterization of the structural, physical, and chemical properties and their functions in various field of technology, is a fundamental cornerstone of nanotechnology and nanoscience. The applications of nanoparticles are known in many fields, such as catalysis, coating, semiconductors, pharmaceutical products, and electronics [1]. Among all practical matters that are produced at the nanometer scale, metal oxides are mainly attractive candidates from a technological and scientific point of view. The distinctive characteristics of metal oxides make them the most varied class of materials, and they have properties that cover almost all aspects of solid-state physics and materials science [2]. The use of metal oxide nanoparticles have become promising in solid-state chemistry because of their remarkably varied properties and structures [3]. They display fascinating magnetic and electronic properties. The use of metal oxide nanoparticles is suitable in many applications such as biomedical, catalysis, pharmaceutical products, surface coatings, semiconductors, and in the medical

field. Among all metal oxide nanoparticles, copper oxide has gained the most interest because of its wide applications, such as solar cell technology [4], field emission [5], magnetic storage media [6], application in lithium ion batteries [7], gas sensing [8], drug delivery, magnetic resonance imaging, and field emission devices [9]. Many different physical and chemical methods have been proposed to synthesize CuO (NPs). These methods include quick precipitation [10], thermal decomposition [11], chemical reduction [12], vapor deposition [13], electrochemical [14], and microwave irradiation [15]. Different morphologies have been synthesized by these methods, such as nanosphers [16], nanorods and nanowires [17], nanodendrits [18], and nanoflowers [19]. The quick-precipitation and hydrothermal methods are used most often because they are safe and environmentally friendly [20]. The use of the quick precipitation method is particularly more attractive because of its cost-effectiveness and simple operation. Cupric oxide (CuO) is a transition metal oxide with a p-type semiconducting material, a monoclinic crystal structure, and an indirect band gap (Eg) of 1.0 eV to 2.08 eV [21, 22]. In the synthesis of metal oxide nanoparticles, polymers are used to stabilize the aggregation of metal atoms. Polyvinylpyrrolidone (PVP) is the most commonly used polymer in the preparation of metal oxides because of its distinct shape, dissolved metal salts, and transport facility. In addition, PVP can be kinetically and thermodynamically controlled. Zhang et al. [23] used PVP as a capping agent to synthesize Cu_2O nanocubes. Park et al. [24] utilized PVP to fabricate Cu_2O nanocubes and CuO nanoparticles. According to recent research results, the molar ratio of OH^- can influence the shape and size of the products. Li et al. [25] obtained CuO nanostructures with different sizes and shapes by the quick precipitation method. $Cu(NO_3)_2$ and hexamethylenetetramine ($C_6H_{12}N_4$) were utilized to fabricate CuO nanostructures. The pH of the solution was regulated by adding sodium hydroxide (NaOH) and nitric acid (HNO_3). Substrates (Si or ITO/glass) were also used. The effect of synthesis conditions on the shape of CuO nanoparticles was investigated, and the results indicated that the synthesis temperature, presence of seeds solution concentration, and pH values significantly affected the morphology of the obtained CuO and its adhesion to the substrate. The current study examines well-dispersed CuO nanosheets with controllable sizes and shapes, which were synthesized by the simple quick-precipitation method. In the preparation process, PVP was chosen to function as a stabilizer and NaOH as a reducing agent. Efforts were focused on the changes in size and shape of the obtained CuO nanostructures when the volume ratios of NaOH were varied.

2. Experimental

2.1. Chemical Reagents

All chemicals used in the experiment were analytical reagent grade and were used without further purification. PVP (*Mw* 10,000) was provided by Sigma Aldrich (USA). Copper nitrate trihydrate (98%, $Cu(NO_3)_2.H_2O$ and NaOH (99.5%) pellets were purchased from R&M chemicals (UK). Distilled water was used throughout the experiment.

2.2. Preparation

In a typical experimental procedure, 1.45 g of $Cu(NO_3)_2.H_2O$ was dissolved in 60 mL of PVP 1 wt.%. The solution was added into a round-bottom flask with stirring. The color of the mixture was bright blue. About 15 mL of NaOH (1M) was rapidly added into the mixture, and a nanopowder suspension was

formed. The suspension was kept at 60 °C for 1 h. A large amount of black precipitate was produced. After cooling to room temperature, the particles were separated by centrifugation and were washed with distilled water thrice to remove the impurities. The particles were then dried in an oven at 60 °C.

2.3. Characterization

X-ray diffraction (XRD) was carried out to characterize the structure of the samples. The XRD patterns with diffraction intensity versus 2θ were recorded using XRD, Philips, X′pert, and Cu-Kα radiation. A SHIMADZU UV-1650 spectrometer was used to record the UV-visible absorption spectra of the CuO nanostructures. Transmission electron microscopy (TEM) studies were carried out with HITACHI H-7100. The particle size distributions were determined using the UTHSCSA Image Tool version 3.00 program. Field emission scanning electron microscopy (FESEM) and energy dispersive analysis of X-ray (EDAX) studies were carried out with JEOL JSM-7600F. The compositions of the products were characterized by Fourier transform infrared (FT-IR) spectroscopy with Perkin Elmer 1650.

3. Results and Discussion

3.1. Effect of volume ratio of NaOH

The volume ratio of NaOH has an significant influence on the shape and size of final products. The products were prepared at six volume ratios of NaOH, namely, 1, 2, 5, 10, 15, and 20 mL of NaOH (1 M) to investigate the effect of the volume ratio. Fig. 1 shows the schematic of the process. At the end of the reaction, the pH values of all samples were measured (Table 1).

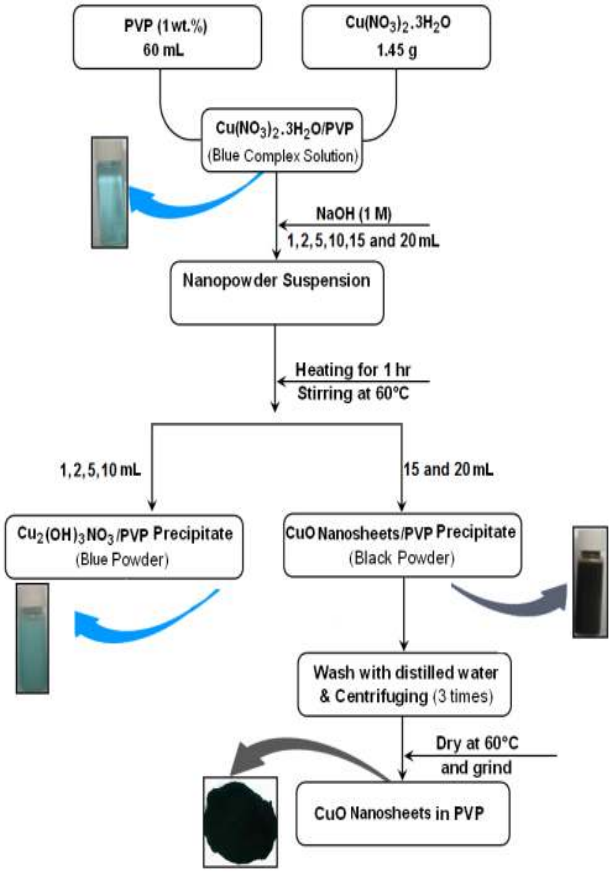

Fig. 1. Flow chart for the synthesis of the CuO nanosheets by the quick precipitation method

Table 1. Characteristic of CuO nanosheets with respect to pH

Sample Names	Volume ratio of NaOH (mL)	pH	λmax (nm)	Color
1	1	4.0	N/A	Blue
2	2	4.1	N/A	Blue
3	5	4.3	N/A	Blue
4	10	5.2	N/A	Blue
5	15	9.7	298, 344	Black
6	20	12.3	285, 342	Black

N/A: Not appeared

Table 1 presents the variants of pH, maximum absorption wavelengths, and colors. The pH was increased from 4 to 12.3 by adding NaOH. At lower pH values, which were equivalent to the addition of 1, 2, 5, and 10 mL of NaOH, the color of the solutions became pale blue. However, at higher pH values, which were equivalent to the addition of 15 and 20 mL NaOH , the color of solution became intense blue then changed in situ into black. A black color indicates the formation of CuO nanoparticles. The pH values moderately increased with the addition of 1, 2, 5, and 10 mLo of NaOH, and significantly increased after the addition of 15 mL of NaOH. In the absorption wavelength (λ_{max}) of the column, no peak was observed at low pH values. However, at higher pH values, two peaks were observed at 298 and 344 nm in 15 mL and 285 and 342 nm in 20 mL, respectively. Fig. 2 shows the UV-vis spectra of all samples shown in Table 1. These results illustrate that the formation of CuO nanostructures did not occur at lower pH values.

Fig. 1 shows the XRD pattern of the obtained samples at different volume ratios of NaOH (1, 2, 5 10, 15, and 20 mL). XRD confirmed the existence of $Cu_2(OH)_3NO_3$ at lower pH values (see Fig. 1a-d). This result shows that pure CuO was not formed in these volume ratios, whereas at higher pH values, the formation of pure CuO was observed (see Figs. 1e and f). All diffraction peaks can be indexed as the monoclinic phase of CuO. This result demonstrate that the reaction at lower pH values could not be completed; however, an excess amount of NaOH resulted in a complete reaction.

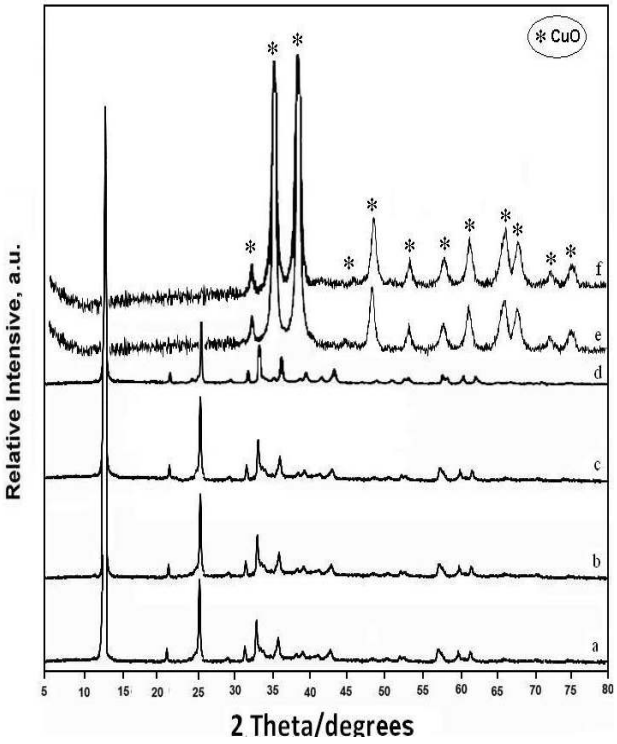

Fig.1 XRD patterns at different volume ratios of NaOH, (a) 1; (b) 2; (c) 5; (d) 10; (e) 15and (f) 20 mL

Fig. 2 illustrates the optical absorption characteristics of CuO nanostructures at different volume ratios of NaOH. No peak was observed at lower pH values, whereas two peaks at 298 and 344 nm in 15 mL and 285 and 342 nm in 20 mL were observed. This result confirms the formation of CuO nanostructures. The two peaks observed in each curve could be attributed to the existence of two different shapes or sizes of the nanoparticles.

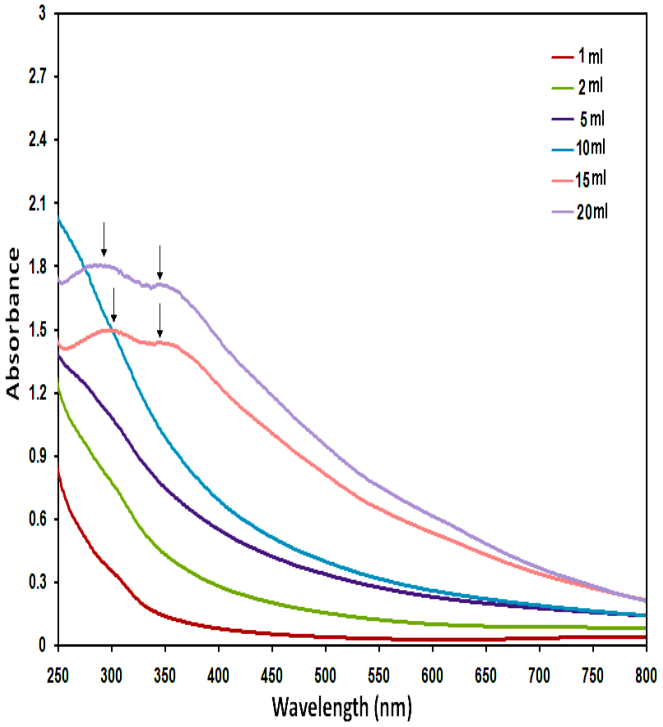

Fig.2 The UV–vis absorption spectra of PVP 1% with different volume ratio of NaOH

Fig. 3 illustrates the TEM micrographs of CuO nanostructures prepared at different volume ratios of NaOH. Figs. 3a and 3b show the results for the addition of 15 and 20 mL of NaOH, respectively. These figures show that sheet-like CuO was formed with a thickness of 175 ± 62 nm and a length of 353 ± 227 nm for 15 mL of NaOH and a thickness of 156 ± 82 nm and length of 742 ± 234 nm for 20 mL of NaOH. Fig. 3(a) also reveals a proportion of the rod-like CuO (rod-like indicated by arrows) among the products.

The high magnification image of the CuO nanosheets prepared in 15 mL is shown in Fig. 4. This image reveals that each sheet-like particle is composed of rod-like particles (indicated by arrows). The reason for the formation of sheet-like CuO from CuO nanorods can be described based on the oriented attachment mechanism. In this process, a larger crystal structure is formed from small ones by the direct joint of suitable crystal planes [26] because the formation of larger crystals can significantly reduce the interfacial energy of some primary nanoparticles.

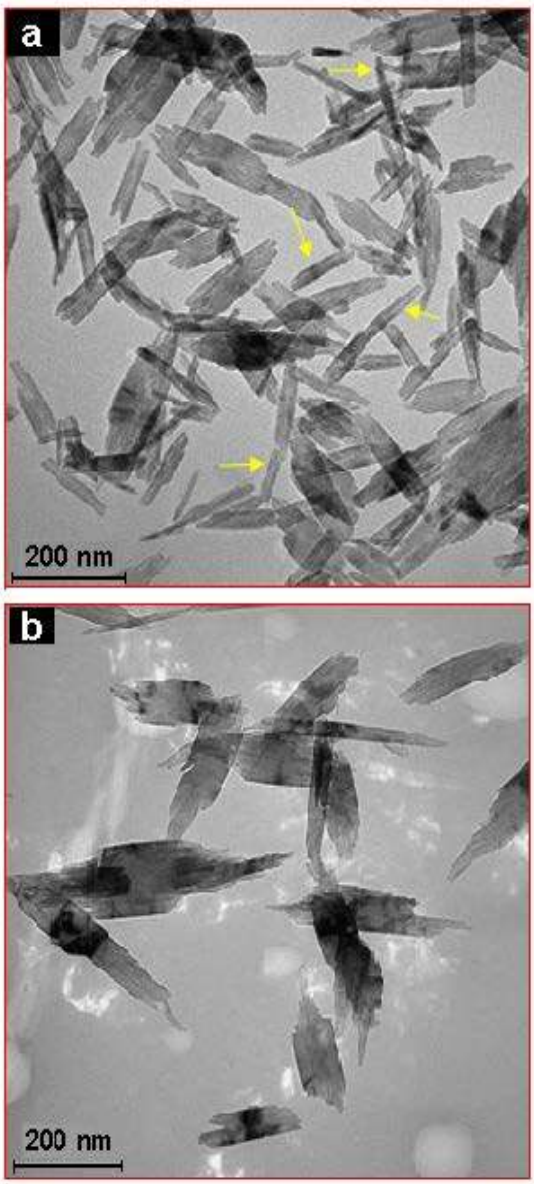

Fig.3 The TEM images of CuO nanosheets in different volume ratio of NaOH 1M. (a) 15 (b) 20 mL

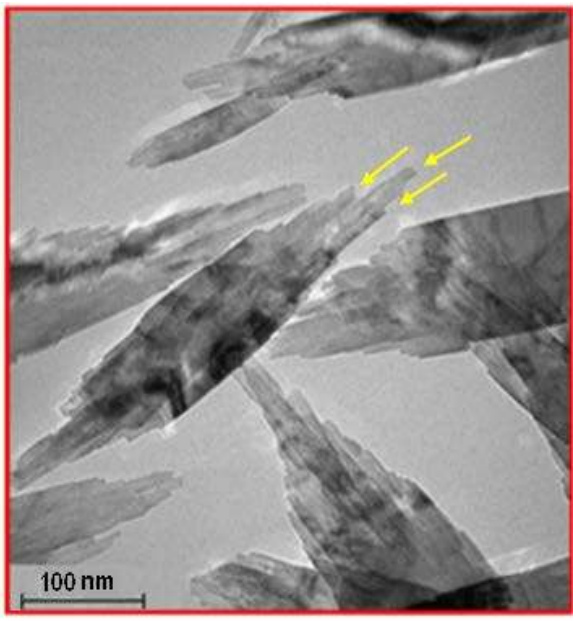

Fig.4 The high magnification TEM images of CuO nanostructures prepared in 15 mL NaOH

The morphology of the products prepared with the addition of 15 and 20 mL of NaOH is shown in Figs. 5a and 5b. The results indicate that sheet-like CuO were formed. Fig. 5a also reveals a proportion of the rod-like CuO (indicated by arrows) among the products. Fig. 5a confirms that the oriented attachment (OA) mechanism is the reason for the formation of sheet-like CuO, which is similar to the synthesis of CuO hierarchical nanostructures. In this mechanism, smaller particles are joined side by side to form sheet-like structure. Fig. 5b shows the surface morphology of the sample obtained with the addition of 20 mL of NaOH. This image shows that with the addition of 20 mL, only sheet-like CuO were formed and no rod-like CuO was observed.

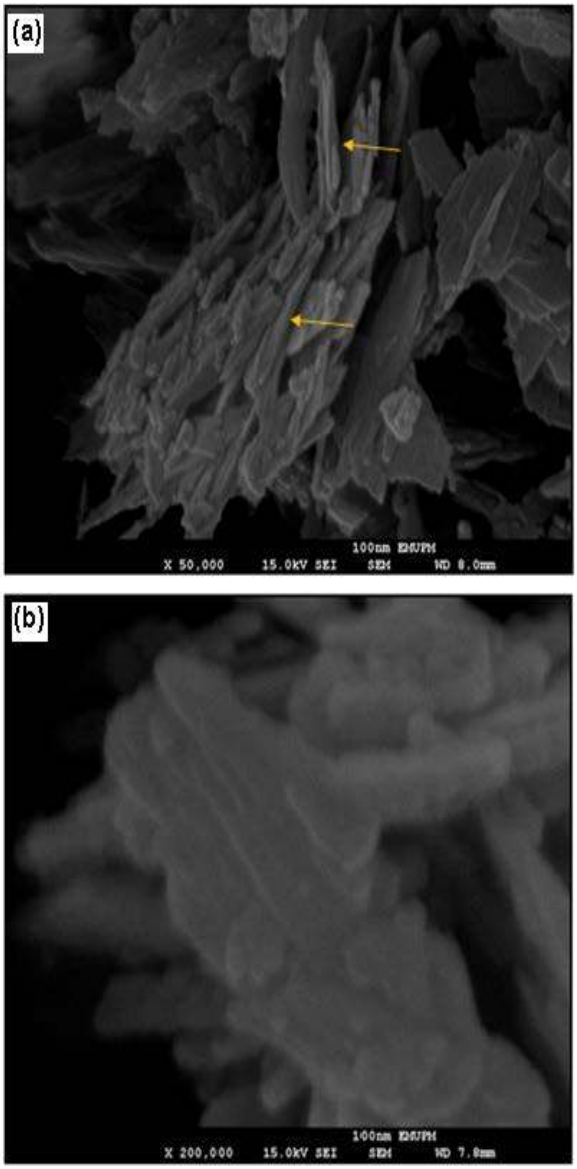

Fig.5 FE-SEM micrograph of products obtained in addition of 15 mL in PVP 1 wt% (a) and in addition of 20 mL (b)

EDAX was carried out on the obtained CuO nanosheets at 15 KeV by using FE-SEM. The EDAX spectrum (Figs. 5a and 5b) related to the CuO nanosheets obtained in 1 wt.% PVP with the addition of 15 and 20 mL of NaOH obviously confirms the presence of Cu and O peaks. The result of EDAX also confirms that the atomic ratio of Cu to O is 1:1. The specimens were coated by gold (Au) before FE-SEM observation.

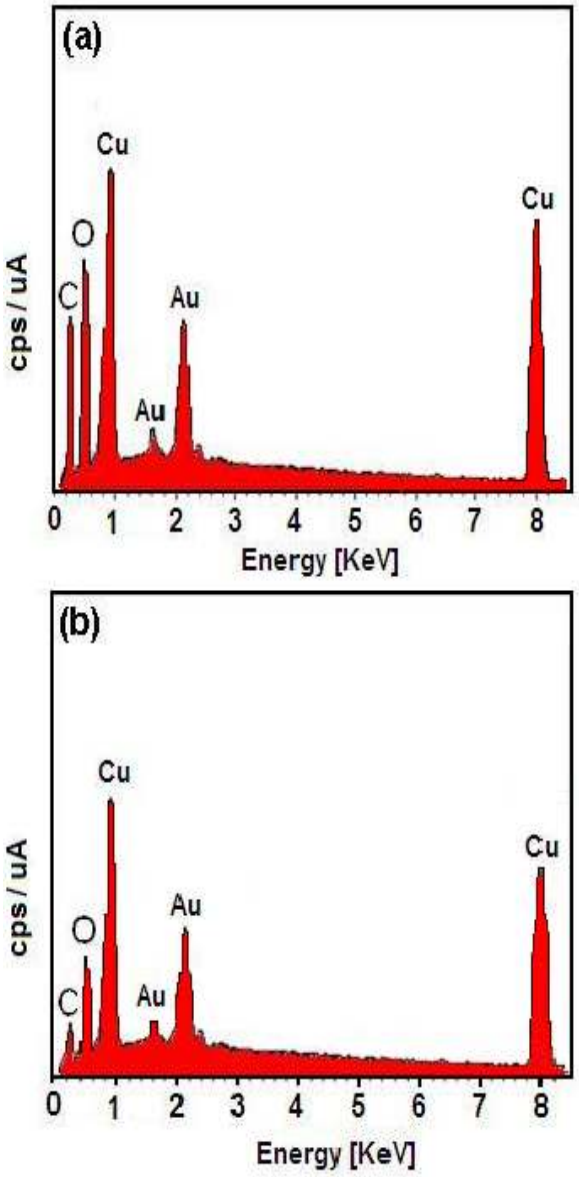

Fig.6 EDX spectra of CuO nanosheets obtained in PVP 1 wt% in addition of 15 (a) 20 mL (b)

FT-IR is a suitable and sensitive method to detect the interaction between two species [27]. FT-IR was carried out to confirm if the CuO nanosheets were modified by PVP. Fig. 6 shows the FT-IR spectra for pure PVP (Fig. 6a), CuO nanosheets produced in 15 mL of NaOH (Fig. 6b), and CuO nanosheets produced in 20 mL of NaOH (Fig. 6c). In the FT-IR spectrum of pure PVP, the peak at 1662 cm^{-1} corresponds to the peak of C=O. In contrast to the curve (Fig. 6a) with another treatment condition, the results show that the peak of C=O shifted to 1649 (Fig. 6b) and 1642 cm^{-1} (Fig. 6c) in the FTIR spectra of the CuO nanosheets. These results indicate the existence of weak chemical bonds between the band of C=O and CuO nanosheets [28]. Metal oxide commonly has absorption bands below 1000 cm^{-1} [29]. The absorption bands observed at 600 and 505 cm^{-1} in Fig. (6b) and absorption bands at 601 and 483 cm^{-1} in Fig. (6c) were characteristic of Cu–O.

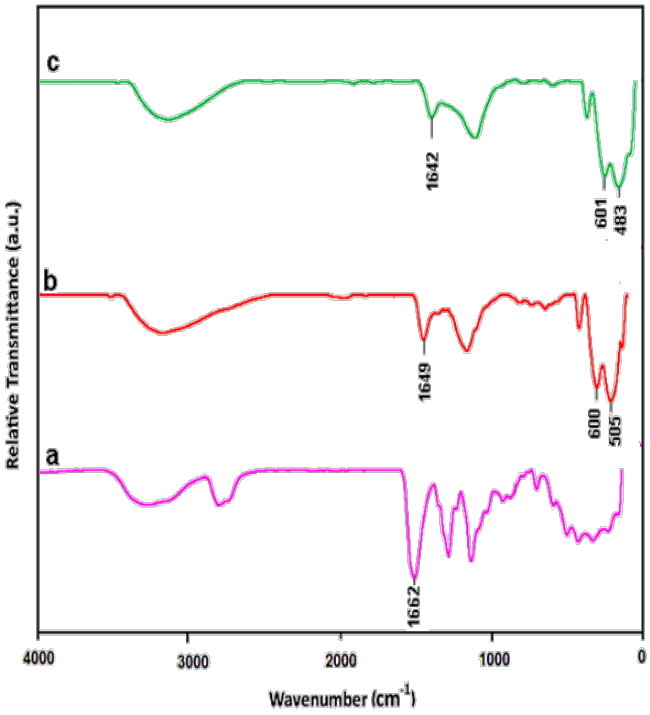

Fig.7 The FT-IR spectra of samples, pure PVP (a) CuO nanosheets obtained with NaOH 15 mL (b), 20 mL (c)

3.2. Mechanism

A number of the most primitive methods to synthesize nanoparticles were carried out by

the precipitation of sparsely soluble components from aqueous solutions, followed by thermal decomposition of those soluble components to oxides. This method has become very common in synthesizing metallic and semiconducting oxide nanoparticles. This method consists of four steps, which include the formation of the precursor, nucleation, growth, and aging [30]. The process can be explained in a simple form. The fabrication of precursor molecules generally occurs through hydrolysis reactions and hydroxylation to form a zero-charge molecule. The formation of precursor molecules causes a supersaturation, which is defined as a state in which the liquid (solvent) contains more dissolved solids (solute). Supersaturation functions as a driving force for crystallization. When supersaturation occurs, a nucleus is formed and precipitation starts. The nuclei is described as the smallest solid phase that aggregates from ions, atoms or molecules formed during the precipitation process and has the ability to grow spontaneously. When the precursor concentration is above the crucial concentration of nucleation, new particles are produced. When the precursor concentration drops below the crucial concentration because of the using precursors during the growth process, only the particle growth of the present particles is retained. After nucleation and growth, the particle morphology, particle size, and size distribution of the produced nanoparticles might change by aging [31]. The aging process consists of two main events, namely, aggregation and coarsening (also known as Ostwald ripening).

In our case, we proposed the following mechanism for CuO nanosheet growth: when a small amount of NaOH was added to a solution (1, 2, 5, and 10 mL), a pale blue $Cu_2(OH)_3NO_3$ precipitate formed instead of $Cu(OH)_2$ (Eq. 1). This result can be attributed to the solubility product of $Cu_2(OH)_3NO_3$ that reaches the precipitation limit before that of Cu $(OH)_2$. When a higher amount of NaOH was added to the solution (15 or 20 mL), an intense blue $Cu(OH)_2$ formed (Eq. 2), which indicates that supersaturation occurred because of hydroxylation. Nucleation immediately occurred after supersaturation. In the nucleation step, a growth unit was needed for the crystals to grow on. The anionic coordinative polyhedral theoretical model is used to explain the growth mechanism. Based on this model, the cations are considered to exist in a form of a complex, whose ligands are OH^- ions in an aqueous solution and also form complexes with coordinative numbers that are equal to that of the formed crystal. Furthermore, cations are identified as a growth unit. In aqueous solutions, the coordination number of Cu^{2+} is normally six [32]. Consequently, growth units exist in $Cu(OH)_6^{4-}$ of the coordinating octahedron in the NaOH solution. In a $Cu(OH)_6^{4-}$ complex, two OH^- ligands are located at its axis, and four OH^- ligands are located at the square plane. The binding energies of four OH^- ligands are higher than the two axial ligands because of the interplane distances are shorter compared with that of the two axial OH^-. Therefore, the two axial OH^- ligands are easily dehydrated to form anisotropic CuO nanoparticles. The introduction of selective capping agents, such as PVP, can control the growth rates of various faces of metal oxide nanoparticles throughout the adsorption on these surfaces. PVP macromolecules can selectively interact with different faces of CuO nanostructures through Cu–N and Cu–O coordination bonds [33]. In the absence of PVP, CuO nuclei randomly grow into irregular shapes. In this case, the oxygen atoms of PVP is bound to the CuO. Another major component in this process is the reaction temperature. At low temperatures,

the $Cu(OH)_6^{4-}$ complex formed hydrogen bonds, which can stabilize this complex at low temperatures. When the temperature was increased, the hydrogen bonds were demolished, and the growth units of $Cu(OH)_6^{4-}$ were rapidly destroyed. Finally, black CuO nanostructures were formed (Eq. 3).

$$2[(Cu(NO_3)_2(PVP)]+3NaOH \xrightarrow{\text{Low pH}} Cu_2(OH)_3NO_3(PVP)+3NaNO_3 \quad (1)$$

$$[(Cu(NO_3)_2(PVP)]+NaOH \xrightarrow{\text{high pH}} Cu_2(OH)_2(PVP)+3NaNO_3 \quad (2)$$

$$Cu(OH)_2\,(PVP) \xrightarrow{\Delta} CuO\,(PVP) + H2O \quad (3)$$

4. Conclusion

CuO nanosheets were successfully synthesized in PVP by using the quick precipitation method at a low reaction temperature (60 °C) in the absence of templates and additives. The results illustrated that pure CuO nanostructures were formed only at higher pH values. FT-IR results showed that PVP interacted with CuO nanostructures through the Cu–O coordination bond. The TEM results show that sheet-like CuO structures were formed with a thickness of 175 ± 62 nm and a length of 353 ± 227 nm with the addition of 15 mL of NaOH and a thickness of 156 ± 82 nm and length of 742 ± 234 nm with the addition of 20 mL of NaOH. In conclusion, CuO nanostructures were not formed because supersaturation did not occur at low pH values.

5. Acknowledgment

Thanks are due to Dr. Nabi Motallebi for helpful discussion and ideas. The authors are also grateful to staff of Microscopy unit of Institute of Bioscience UPM for technical support.

References:

[1] V. Saez, T.J. Mason, Sonoelectrochemical synthesis of nanoparticles, *Molecules*, 14, 2009, pp. 4284-4299.

[2] M. Niederberger, N. Pinna, *Metal Oxide Nanoparticles in Organic Solvents: Synthesis, Formation, Assembly and Application*, Springer, 2009.

[3] N. Imanaka, T. Masui, Particles and Single Crystals of Rare Earth Oxides, *Binary Rare Earth Oxides*, 37, 2005, pp. 135-161.

[4] H. Zhang, M. Zhang, Synthesis of CuO nanocrystalline and their application as electrode materials for capacitors, *Materials Chemistry and Physics*, 108, 2008, pp.184-187.

[5] X. Zhang, D. Zhang, X. Ni, H. Zheng, Optical and electrochemical properties of nanosized CuO via thermal decomposition of copper oxalate, *Solid-State Electronics*, 52, 2008, pp. 245-248.

[6] N. Topnani, S. Kushwaha, T. Athar, Wet Synthesis of Copper Oxide Nanopowder, International Journal of Green Nanotechnology: *Materials Science & Engi*neering, 1, 2009, pp. 67-73.

[7] S. Seung-Deok ,J. Yun-Ho ,L. Seung-Hun ,S. Hyun-Woo ,K. Dong-Wan, Low-temperature synthesis of CuO-interlaced nanodiscs for lithium ion battery electrodes, *Nanoscale Research Letters*, 6, 2011, pp. 2-7.

[8] X. Gou ,G. Wang ,J. Yang ,J. Park ,D. Wexler, Chemical synthesis, characterization and gas sensing performance of copper oxide nanoribbons, *J. Mater. Chem.*, 18, 2008, pp. 965-969.

[9] M.A. Dar ,Y.S. Kim ,W.B. Kim ,J.M. Sohn ,H.S. Shin, Structural and magnetic properties of CuO nanoneedles synthesized by hydrothermal method, *Applied Surface Science*, 254, 2008, pp. 7477-7481.

[10] J. Zhu, D. Li, H. Chen, X. Yang, L. Lu, X. Wang, Highly dispersed CuO nanoparticles prepared by a novel quick-precipitation method, *Materials Letters*, 58, 2004, pp. 3324-3327.

[11] Y.H. Kim, D.K. Lee, B.G. Jo, J.H. Jeong, Y.S. Kang, Synthesis of oleate capped Cu nanoparticles by thermal decomposition, *Colloids and Surfaces A: Physicochemical and Engineering Aspects*, 284, 2006, pp. 364-368.

[12] A.A. Athawale, P.P. Katre, M. Kumar, M.B. Majumdar, Synthesis of CTAB-IPA

reduced copper nanoparticles, *Materials chemistry and physics*, 91, 2005, pp. 507-512.
[13] A.A. Ponce, K.J. Klabunde, Chemical and catalytic activity of copper nanoparticles prepared via metal vapor synthesis, *Journal of Molecular Catalysis A: Chemical*, 225, 2005, pp. 1-6.
[14] Z. Zhang, P. Wang, Highly stable copper oxide composite as an effective photocathode for water splitting via a facile electrochemical synthesis strategy, *J. Mater. Chem.*, 22, 2012, pp. 2456-2464.
[15] H.T. Zhu, C.Y. Zhang, Y.M. Tang, J.X. Wang, Novel synthesis and thermal conductivity of CuO nanofluid, *The Journal of Physical Chemistry C*, 111, 2007, pp. 1646-1650.
[16] J. Zhang, J. Liu, Q. Peng, X. Wang, Y. Li, Nearly monodisperse Cu_2O and CuO nanosphers: preparation and applications for sensitive gas sensors, *Chemistry of materials, 18, 2006,* pp. 867-871.
[17] R. Shende, S. Subramanian, S. Hasan, S. Apperson, R. Thiruvengadathan, K. Gangopadhyay, Nanoenergetic Composites of CuO Nanorods, Nanowires, and Al-Nanoparticles, *Propellants, Explosives, Pyrotechnics*, 33, 2008, pp. 122-130.
[18] S. Li, H. Zhang, Y. Ji, D. Yang, CuO nanodendrits synthesized by a novel hydrothermal route, *Nanotechnology*, 15, 2004, pp. 1428-1432.

[19] Z. Yang, J. Xu, W. Zhang, A. Liu, S. Tang, Controlled synthesis of CuO nanostructures by a simple solution route, *Journal of Solid State Chemistry,* 180, 2007, pp. 1390-1396.
[20] D. Li, Y.H. Leung, A.B. Djurisic, Z.T. Liu, M.H. Xie, J. Gao, W.K. Chan, CuO nanostructures prepared by a chemical method, *Journal of crystal growth*, 282, 2005, pp. 105-111.
[21] J. Jun, C. Jin, H. Kim, S. Park, C. Lee, Fabrication and characterization of CuO-core/TiO< sub> 2</sub>-shell one-dimensional nanostructures, *Applied Surface Science*, 255, 2009, pp. 8544-8550.
[22] Y. Hao, H. Gong, the Influence of In/Cu Ratio on Electrical Properties of CuO: In Thin Films Prepared by Plasma Enhanced CVD, *Chemical Vapor Deposition*, 14, 2008, pp. 9-13.
[23] H. Zhang, Z. Cui, Solution-phase synthesis of smaller cuprous oxide nanocubes, *Materials Research Bulletin*, 43, 2008, pp. 1583-1589.
[24] J. C. Park, J. Kim, H. Kwon, H. Song, Gram-Scale Synthesis of Cu2O Nanocubes and Subsequent Oxidation to CuO Hollow Nanostructures for Lithium Ion Battery Anode Materials, *Advanced Materials*, 21, 2009, pp. 803-807.
[25] D. Li, Y. H. Leung, A.B. Djurisica, Z.T. Liua, M.H. Xiea, J. Gaoa, W.K. Chanb, CuO nanostructures prepared by a chemical method, *Journal of crystal growth*, 282, 2005, pp. 105-111.
[26] R.L. Penn, J.F. Banfield, Imperfect oriented attachment: dislocation generation in defect-free nanocrystals, *Science*, 281, 1998, pp. 969-971.
[27]. W. Tu, X. Zuo, H. Liu, Study on the Interaction between Polyvinylpyrrolidone and Platinum Metals during the Formation of the Colloidal Metal Nanoparticles, *Chinese Journal of Polymer Science*, 26, 2008, pp. 23-29.
[28]. J. Bai, Y. Li, L. Sun, C. Zhang, Q. Yang, Bicomponent AgCl/PVP nanofibre fabricated by electrospinning with gel-sol method, *Bulletin of Materials Science*, 32, 2009, pp. 161-164.
[29]. C.N.R. Rao, *Chemical applications of infrared spectroscopy*, Academic Press, 1963.
[30] J.P. Jolivet, M. Henry, J. Livage, *Metal oxide chemistry and synthesis: from solution to solid state*, John Wiley, 2000.
[31] G. Oskam, Metal oxide nanoparticles: synthesis, characterization and application, *Journal of sol-gel science and technology*, 37, 2006, pp. 161-164.
[32] M. Arthur Earl, R.D. Hancock, *Metal complexes in aqueous solutions*, Plenum Press, 1996.
[33] H. Zhang, Z. Cui, Solution-phase synthesis of smaller cuprous oxide nanocubes, *Materials Research Bulletin*, 43, 2008, pp. 1583-1589.